

Luminescent Glass-Ceramics Based on Nanoparticles of $\text{Ba}_x\text{RE}_{1-x}\text{F}_{2+x}$ and $\text{Pb}_x\text{RE}_{1-x}\text{F}_{2+x}$ Solid Solutions into Fluoroborate

Olga Petrova, Tatjana Sevostjanova, Andrew Khomyakov, and Igor Avetisov*

Lead-barium fluoroborate glasses doped with RE are synthesized. Using the heat-treatment (HT) glass-ceramics in which RE^{3+} (Eu^{3+} or Er^{3+}) ions are building into fluoride crystalline nanoparticles homogeneously distributed in the borate glass matrix are made. The changes in the structural and optical properties of the glass-ceramics comparatively to initial glasses and polycrystalline fluoride containing Pb, Ba, and RE are revealed by X-ray diffraction and luminescence spectroscopy of RE ions.

1. Introduction

Oxyfluoride glass-ceramics (GCs) are widely researched as host materials for active optical ions because they have not only comparatively low phonon energies which corresponding to fluoride crystals, but also high chemical and mechanical stabilities related to oxide glasses. Due to fluorine depletion these systems are characterized by self-restriction of fluoride crystallite size growth. Thus, it is possible to obtain monodimension nanocrystals homogeneously distributed in a glass matrix, which provide high transparency of GCs.

In lead fluoroborate,^[1–4] barium fluoroborate,^[5] and mixed^[6] systems it's possible to get RE doped glasses.

The $\text{PbF}_2\text{--PbO--B}_2\text{O}_3$ system is characterized by a very broad glass transition range; the glasses have low synthesis and glass transition temperatures, relatively low hardness, high density, high refractive index, and ionic conduction. In this system glass crystallization follows by the formation of two fluoride crystalline phases, namely, the low-temperature orthorhombic $\alpha\text{-PbF}_2$ (*Pnam*) phase and the high-temperature cubic $\beta\text{-PbF}_2$ (*Fm3m*) phase. Rare-earth dopants efficiently intercalate into the $\beta\text{-PbF}_2$ phase,^[4] whereas $\alpha\text{-PbF}_2$ is a parasitic phase, which considerably increases optical losses due to its birefringence.

In the $\text{BaF}_2\text{--BaO--B}_2\text{O}_3$ system comparing to the $\text{PbF}_2\text{--PbO--B}_2\text{O}_3$ system, the glass transition range is narrower, the synthesis and glass transition temperatures are higher, and the glasses have higher hardness and lower refractive index. The produced glasses contain only the cubic crystalline phase BaF_2 (*Fm3m*), but

rare-earth dopants hardly dissolve in this phase^[5] (Tables S1 and S2, Supporting Information).

In a mixed system, depending on the composition and crystallization conditions one may obtain phases of different compositions, including the cubic phase $\text{Pb}_x\text{Ba}_{1-x}\text{RE}_y\text{F}_{2+y}$ solid solution with a high RE concentration.^[6]

We have chosen, Er and Eu as dopants, because they are simultaneously widely applicable activators for phosphors and lasers as well as good probes for testing the

change in the structure of the material. Materials activated by Eu^{3+} are effective red phosphors, and the number, splitting and the ratio of the emission lines in the Eu^{3+} luminescence spectrum makes it possible to determine the structure and symmetry of optical centers.^[7–9] For materials activated by Er^{3+} ions, anti-Stokes luminescence can be observed in the 550 and 650 nm at 975 nm excitation, caused by the mechanisms of up-conversion and/or absorption from the excited state.^[10] The efficiency of the up-conversion is related to the phonon spectrum of the material and the distance between the Er^{3+} ions. Thus, the appearance, change in intensity and redistribution of intensity between anti-Stokes luminescence bands can indicate changes in the structure of the material, and materials with effective anti-Stokes luminescence can be used as phosphors (e.g., infrared visualizer) and lasers.

2. Experimental Section

2.1. Synthesis of Glass-Ceramics

2.1.1. Glass Precursor Synthesis

Samples of glasses in the systems $\text{PbF}_2\text{--PbO--B}_2\text{O}_3$; $\text{BaF}_2\text{--BaO--B}_2\text{O}_3$; $\text{PbF}_2\text{--BaO--B}_2\text{O}_3$; $\text{PbO--BaF}_2\text{--B}_2\text{O}_3$; $\text{PbF}_2\text{--BaF}_2\text{--B}_2\text{O}_3$ nominally pure and 1 mol% doped by RE (Eu or Er) fluorides have been synthesized from B_2O_3 , PbF_2 , BaF_2 , PbO , BaCO_3 , EuF_3 , and ErF_3 not less than 99.90 wt% purity purchased from Aldrich. The batch was 10 g. The glasses were melted in closed corundum crucibles for 0.25–0.5 h at 900–1150 °C in fluorinating atmosphere producing by vaporization of Teflon plates. The amount of Teflon was found out experimentally.^[11] The melt was poured into heated steel or duralumin molds. The compositions with the highest proportion of fluoride components in which optically high-quality glasses were obtained under experiment

Dr. O. Petrova, T. Sevostjanova, A. Khomyakov, Prof. I. Avetisov
Dmitry Mendeleev University of Chemical Technology of Russia
Miuskaya sq. 9, 125047 Moscow, Russia
E-mail: igor_avetisov@mail.ru

DOI: 10.1002/pssa.201700446

conditions were chosen for the further studies. Mixed lead-barium glasses with a good optical quality were synthesized only from a batch with a boron oxide concentration no lower than 50 mol%. The glass compositions and their properties are presented in Table 1. The samples were made as 5–7 mm thick plates. After synthesis, the glasses were annealed at glass transition temperature for 2 h and their basic properties were measured.

2.1.2. Synthesis of Glass-Ceramics

The GCs were produced by heat treatment of glasses under different temperature – time regimes. The temperature range of heat treatments was chosen starting from T_g to the peak of crystallization of the appropriate composition. The transparency of the glass material is affected by the differences in the refractive indices of crystallites and residual glass, the symmetry, dimension, and concentration of crystalline particles. We obtained transparent, semi-transparent, and non-transparent GCs. Non-transparent GCs were unpromising as luminescence matrix and they have not been investigated.

2.1.3. Synthesis of Reference Samples of Crystalline Solid Solutions

The polycrystalline samples of solid solutions of the $Pb_xBa_{1-x-y}RE_yF_{2+y}$ (RE = Eu or Er, $x = 0, 0.2, 0.4, 0.6, 0.8, 1$; $y = 0.01, 0.05, 0.1, 0.2$) were synthesized by the solid-phase method in fluorinating atmosphere in several stages with grinding of the sintered mixture at the every stage. The amount of Teflon was chosen experimentally in such a way that there was no formation of oxide phases during the synthesis according to the X-ray diffraction analysis. The single-phase composition and the

fluorite structure of the samples were confirmed by X-ray diffraction analysis.

2.2. Measurement Techniques

The glassforming, crystallization, and beginning of the melting range were determined by the differential thermal method (DTA). Volatilization of the glass components at heat treatments determined by the thermogravimetric analysis. The heating rate was 10 K min^{-1} . We used a MOM Q-1500D derivatograph with platinum crucibles for DTA. Softening point and thermal expansion coefficient were measured by a quartz dilatometer. The density was measured by hydrostatic weighing, the microhardness was determined by the Vickers method using a PMT-3 microhardness tester, and the refractive index was determined by the Lodochnikov technique on the polarization microscope MIN-8 with a Fedorov table and light filters as described in.^[12]

Elemental analysis was performed on a JSM-5910-LV setup, which combined the functions of a scanning electron microscope and an X-ray spectral microanalyzer. X-ray diffraction analysis was performed with a D2 Phaser (Bruker AXS Ltd.) diffractometer (CuK_α radiation, $\lambda = 1.54060 \text{ \AA}$) within the range of 2θ angles from 10° to 70° at a scan step of 0.01° and an exposure of 2 s step^{-1} . The data were accumulated and processed with EVA and TOPAS software (ver. 2.4).

The absorption spectra of glasses and GCs were recorded on a UNUCO 2800 (UV/VIS) spectrophotometer in 190–1100 nm range. A Fluorolog FL3-22 spectrofluorimeter (Horiba Jobin Yvon, USA) with double grating excitation and emission monochromators has been used for luminescent measurements of europium- and erbium-doped materials in a wavelength range of 400–700 nm with a 0.1 nm step. The emission Eu^{3+} were

Table 1. Compositions and properties of glasses.

Physics properties	Composition of charge, mol%							
	25 BaF ₂ 25 BaO 50 B ₂ O ₃	35 BaF ₂ 15 PbF ₂ 50 B ₂ O ₃	30 BaF ₂ 20 PbO 50 B ₂ O ₃	20 PbF ₂ 30 BaO 50 B ₂ O ₃	25 BaF ₂ 25 PbO 50 B ₂ O ₃	25 PbF ₂ 25 BaO 50 B ₂ O ₃	45 PbF ₂ 5 BaO 50 B ₂ O ₃	25 PbF ₂ 25 PbO 50 B ₂ O ₃
Glassforming temperature, T_g , °C, ±5	488	336	419	436	411	433	367	347
Crystallization temperature, T_c , °C, ±5	551	542	546	545	533	540	453, 538	442, 547
Softening point T_f , °C, ±5	548	405	437	500	452	483	438	423
Thermal expansion coefficient, $\text{K}^{-1} \cdot 10^{-6}$, ±5 · 10 ⁻⁷	11	10	12	11	12	12	12	13
Escape of fluorine, % of the original, ±5%	12	20	24	28	25	29	40	31
Density, $\text{g cm}^{-3} \pm 0.05$	3.47	3.59	4.07	4.24	4.27	4.10	4.55	5.42
Micro-hardness, $\text{kg mm}^{-2} \pm 10$	511	430	425	443	420	412	309	363
Number of RE ³⁺ ions 10 ²⁰ ions cm ⁻³ (at +1 mol% EuF ₃ or ErF ₃)	1.8	1.9	1.9	1.9	1.9	1.9	1.9	2.1
Short-wave cut of transparency, nm ±5	310	345	350	350	350	350	360	380
Refractive index, n_d , ±0.02	1.59	1.62	1.66	1.69	1.69	1.69	2.08	2.29

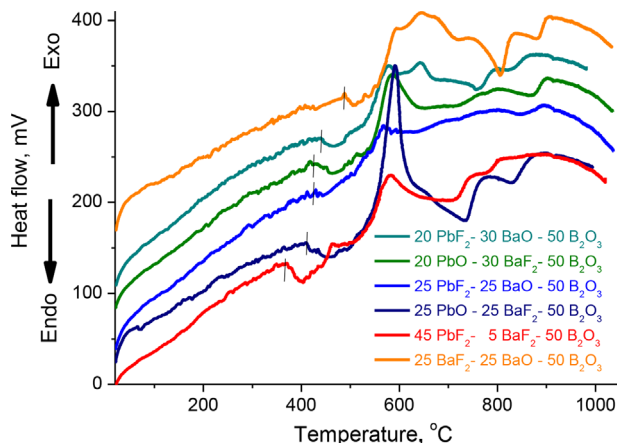


Figure 1. DTA curves of the undoped glasses. The bars indicate T_g .

studied at excitation by a pulsed diode laser ($\lambda = 377$ nm), excited Er^{3+} anti-Stokes luminescence by a 975 nm diode. All luminescence measurements have been carried out at room temperature.

3. Results and Discussion

The investigation of glasses in lead-barium borate systems showed, that parameter's values of mixed glasses occupy an intermediate position between lead and barium fluoroborate glasses' values (Table 1). Density and refractive index increase, characteristic temperatures and microhardness decrease at lead content increase.

As barium concentration increasing in the charge the vaporization of fluorine decreases, while the concentration ratio of Ba and Pb remains almost unchanged for all compositions, which points to low losses of lead fluoride. Thus, the loss mechanism is associated with the formation of BF_3 , as suggested in Ref. [13].

All produced glasses were spontaneously doped by Al (from 3 to 5 wt%) because of the partial dissolving of the corundum crucible by the melt. Incorporation of aluminum into a glass should not negatively affect its spectral and luminescent properties and crystallization behavior, but improve glass mechanical properties,^[14] can enhance the fluorine retention in the melt^[15] and improve the dopant distribution homogeneity.^[16]

All glasses demonstrated a crystallization peak starting at 530–550 °C with a maximum at 570–590 °C (Figure 1). This peak corresponded to the crystallization of the lead fluoride. The high lead concentration glasses have one more crystallization peak at 430–440 °C.

GCs were obtained by heat-treatment (HT) of the initial glasses in various temperature-time modes, which were chosen from DTA measurements. We did not observed volatilization of the glass components at HT (Figure 2).

According to the XRD analysis (Figure 3) the controlled crystallization of these glasses resulted to the formation of cubic phases of solid solutions of $\text{Ba}_x\text{RE}_{1-x}\text{F}_{2+x}$ and $\text{Pb}_x\text{RE}_{1-x}\text{F}_{2+x}$ or $\alpha\text{-PbF}_2$ orthorhombic phase depending on the composition and

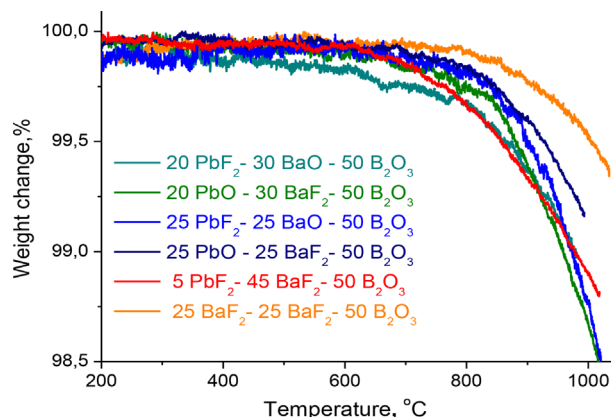


Figure 2. Volatilization of glass components according to thermogravimetric analysis.

conditions (Table 2). Temperatures' increase higher 540 °C resulted to the full destruction of the undesirable $\alpha\text{-PbF}_2$ orthorhombic phase.

The XRD peaks are noticeably broadened; there is a significant glass halo, which indicates that crystalline peaks

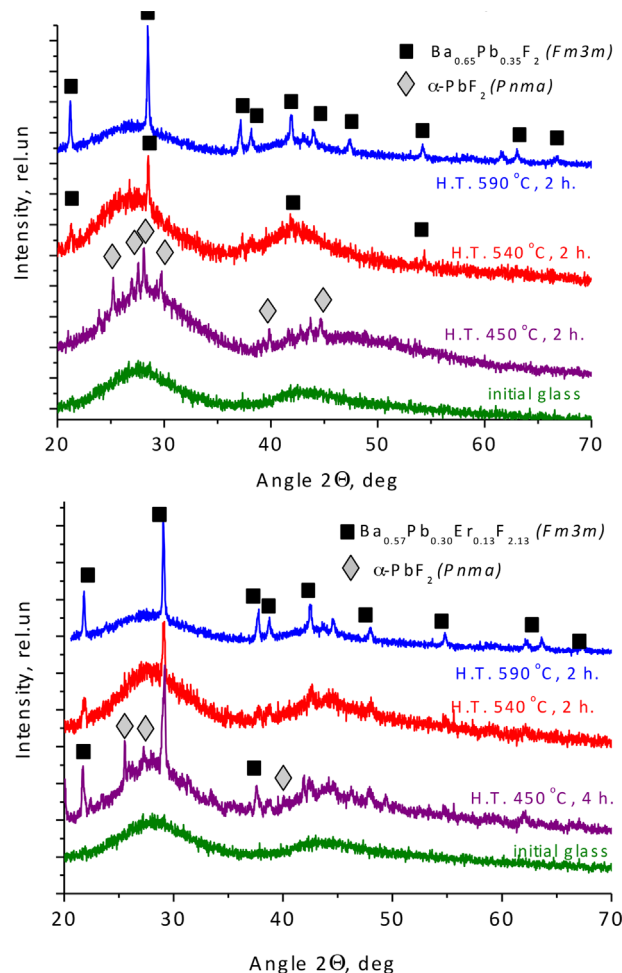


Figure 3. Typical XRD diffraction patterns of glass and GCs obtained from the initial compositions 45PbF₂–5BaF₂–50B₂O₃ (top) and 45PbF₂–5BaF₂–50B₂O₃–1 ErF₃ (bottom).

Table 2. Compositions of crystallizing phases.

Composition of charge, mol%	Conditions of heat treatment, temperature °C / time, h	Composition of crystalline phases
25 PbF ₂ 25 PbO 50 B ₂ O ₃	450/2 540/2	α-PbF ₂ (Pnma) α-PbF ₂ (Pnma)
45 PbF ₂ 5 BaF ₂ 50 B ₂ O ₃	450/2 540/2	α-PbF ₂ (Pnma) Ba _{0.65} Pb _{0.35} F ₂ (Fm3m)
35 BaF ₂ 15 PbF ₂ 50 B ₂ O ₃	450/2 540/2	Pb _{0.4} Ba _{0.6} F ₂ , α-PbF ₂ (Pnma) Pb _{0.4} Ba _{0.6} F ₂ (Fm3m)
25 PbF ₂ 25 BaO 50 B ₂ O ₃	450/2 540/2	Pb _{0.55} Ba _{0.45} F ₂ (Fm3m) Pb _{0.55} Ba _{0.45} F ₂ (Fm3m)
20 PbF ₂ 30 BaO 50 B ₂ O ₃	540/2	Pb _{0.5} Ba _{0.5} F ₂ (Fm3m)
25 BaF ₂ 25 PbO 50 B ₂ O ₃	540/2	Pb _{0.82} Ba _{0.18} F ₂ (Fm3m)
30 BaF ₂ 20 PbO 50 B ₂ O ₃	540/2	Pb _{0.81} Ba _{0.19} F ₂ (Fm3m)

are attributed to the formation of small crystallites inside the amorphous glass.

The compositions of solid solutions were determined using XRD data on crystallites' lattice parameters. The fraction of cubic phase increased at crystallization of the RE doped glasses. RE-dopands effectively dissolved crystallites with a distribution coefficient (K_{eff}) more than 1. The distribution coefficient increased with increasing Pb:Ba ratio in solid solutions: from $K_{\text{eff}} = (7-10)$ at Pb:Ba = 1 up to $K_{\text{eff}} = (12-16)$ at Pb:Ba = 3.

Thus, the formation of solid solutions contained both Ba and RE stabilizes the high-temperature cubic phase of lead fluoride. The addition of RE also stabilizes the cubic phase and this results to the decrease of the content of the orthorhombic phase in the activated GCs (Figure 3 bottom).

The crystallites' size for cubic solid solutions was estimated as 30–40 nm by the Scherrer formula.

Thus, the crystallization peak at 440 °C for glass with high lead concentrations is associated with the formation of the orthorhombic α-PbF₂ (Pnam) phase, despite the fact that this temperature is higher than of α-PbF₂ → β-PbF₂ phase transition temperature 360 °C.^[17]

The GC's extinction spectra (Figure 4) show higher scattering in the visible region compared to the initial glass. The scattering in the GC (HT = 450 °C) containing α-PbF₂ crystalline phases was considerably higher than in GCs with the Ba_{0.57}Pb_{0.30}Er_{0.13}F_{2.13} cubic crystalline phase. This is obviously related to additional scattering due to the birefringence in the orthorhombic α-PbF₂ crystallites. The GC's with cubic phases were characterized by a slight increase in optical losses compared to the initial glasses.

The value of optical losses after partial crystallization for Er-doped and Eu-doped GCs is close.

After glass partial crystallization the luminescence spectrum showed an increase in the relative intensity of the ⁵D₀ → ⁷F₁ transition (Figure 5). This band was the most intense (similar to lanthanum fluoride)^[18] for the polycrystalline preparation which had been synthesized for comparison. The symmetry of the local crystal field of the Eu³⁺ ions was determined by the ratio of ⁵D₀ → ⁷F₁ and ⁵D₀ → ⁷F₂ transitions.

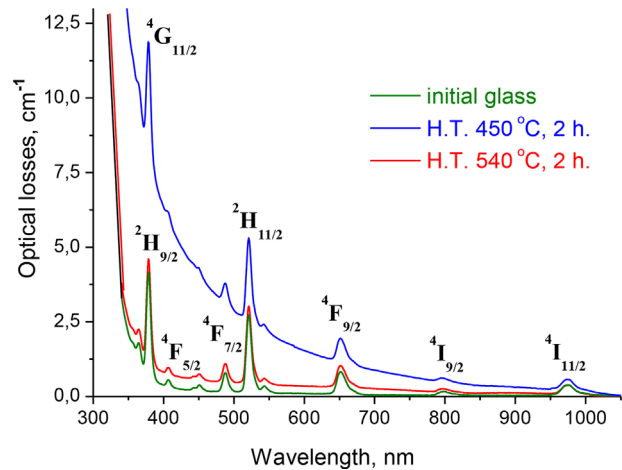


Figure 4. Spectra extinction (optical losses) Er³⁺-doped glass and GC's obtained from the initial composition 45PbF₂–5BaF₂–50B₂O₃–1ErF₃.

The electron dipole transition ⁵D₀ → ⁷F₂ is hypersensitive, and the magneto dipole transition ⁵D₀ → ⁷F₁ is insensitive to a crystal field. In the case of the inversion center the ⁵D₀ → ⁷F₁ (~580 nm) transition is more intense, whereas in the absence of

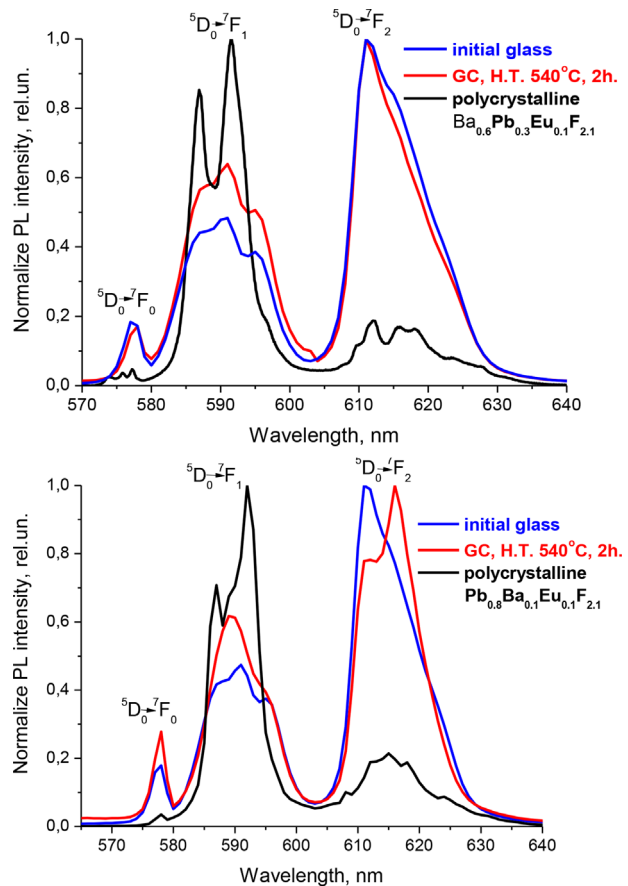


Figure 5. PL spectra of as-synthesized glasses, GCs and polycrystalline fluoride solid solutions, doped Eu³⁺ ($\lambda_{\text{exc}} = 377$ nm), obtained from the initial composition 15PbF₂–35BaF₂–50B₂O₃–1EuF₃ (top) and 25PbO–25BaF₂–50B₂O₃–1EuF₃ (bottom).

Table 3. PL intensities ratio for $^5D_0 \rightarrow ^7F_2$ and $^5D_0 \rightarrow ^7F_1$ transitions.

Luminescent material	The ratio of $^5D_0 \rightarrow ^7F_2 / ^5D_0 \rightarrow ^7F_1$ transition intensities
25 BaF ₂ - 25 PbO - 50 B ₂ O ₃ - 1 EuF ₃	
Initial glass	2,08
GC, H.T. 540 °C, 2h.	1,59
polycrystalline Pb _{0,8} Ba _{0,1} Eu _{0,1} F _{2,1}	0,18
15 PbF ₂ - 35 BaF ₂ - 50 B ₂ O ₃ - 1 EuF ₃	
Initial glass	2,13
GC, H.T. 540 °C, 2h.	1,61
polycrystalline Pb _{0,3} Ba _{0,6} Eu _{0,1} F _{2,1}	0,21

an inversion center the most intense transition is $^5D_0 \rightarrow ^7F_2$ (≈ 612 nm).^[19] Eu centers in lead fluoride have an inversion center. The fraction of these centers increased in GC's in comparison with the initial glass. Thus, the Eu ions effectively dissolved in the crystalline phase (Table 3).

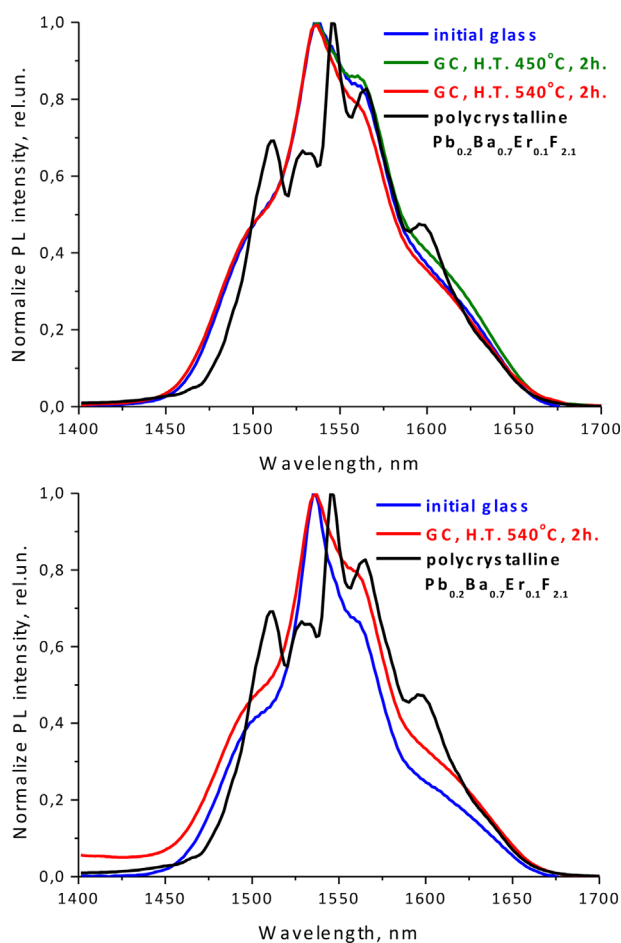


Figure 6. PL spectra transition $^4I_{13/2} \rightarrow ^4I_{15/2}$ of as-synthesized glasses, GCs and polycrystalline fluoride solid solutions, doped Er³⁺ ($\lambda_{\text{ext}} = 973$ nm) obtained from the initial composition 45PbF₂-5BaF₂-50B₂O₃-1ErF₃ (top) and 25PbO-25BaF₂-50B₂O₃-1ErF₃ (bottom).

The IR luminescence spectra of Er³⁺ at the $^4I_{13/2} \rightarrow ^4I_{15/2}$ transition in the GCs (Figure 6) have smooth broad contours. The width of the luminescence band of GC is even wider compared to the initial glass, which corresponds to the band splitting in the case of polycrystalline fluoride Pb_{0,2}Ba_{0,7}Eu_{0,1}F_{2,1}. This type of the band is well matched for telecommunication applications.

In the case of some initial glasses doped by Er³⁺-ions, at IR-excitation (973 nm), we observed a very weak anti-Stokes luminescence in the 665 nm region. We assumed that the population of the upper levels of the Er³⁺-ion has occurred through the mechanism of absorption from the excited state.

According to the XRD data Er was efficiently dissolved into the cubic crystalline phase at HT of the glasses under consideration. It resulted to an intense anti-Stokes luminescence in the 550 and 650 nm regions (Figure 7). The PL intensity sharply increases at crystalline phase fraction growth. Such dependence is typical for an up-conversion mechanism of level occupation. Our previous studies of the dependence of the

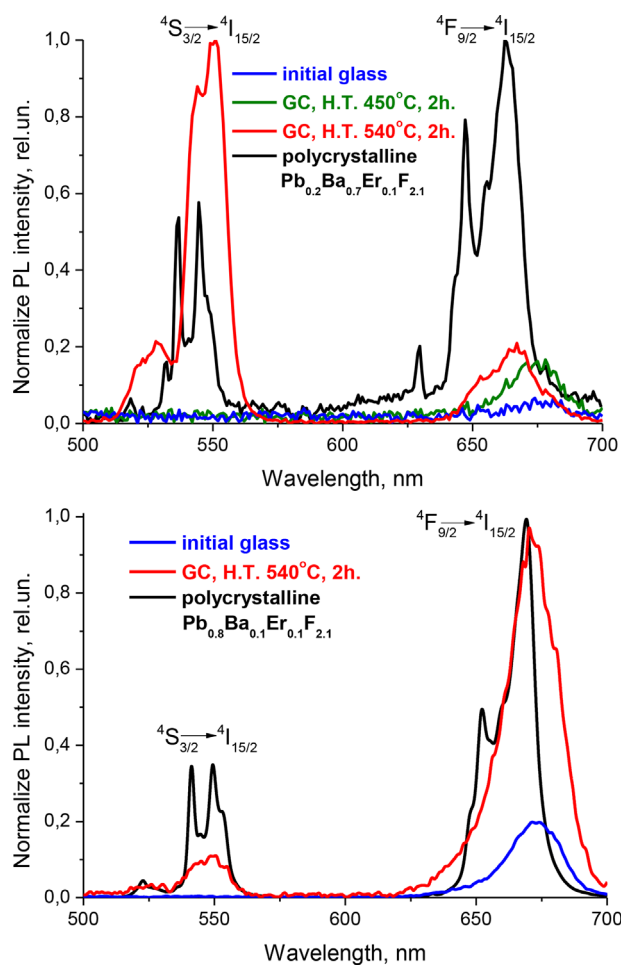


Figure 7. Anti-Stokes PL spectra of as-synthesized glasses, GCs and polycrystalline fluoride solid solutions, doped Er³⁺ ($\lambda_{\text{ext}} = 973$ nm) obtained from the initial composition 45PbF₂-5BaF₂-50B₂O₃-1ErF₃ (top) and 25PbO-25BaF₂-50B₂O₃-1ErF₃ (bottom).

intensity of anti-Stokes luminescence in lead oxyfluoride glasses on the Er concentration showed that such a sharp intensity increase did not occur without a change in the environment of Er^{3+} ions.^[20]

Mechanisms of the anti-Stokes bands (green and red) in Er^{3+} doped materials have been extensively studied elsewhere.^[21] In the case of the green luminescence, two possible routes, namely, the excited state absorption (ESA) and the energy transfer up-conversion (ETU) can be distinguished. In the ESA process, a sequential absorption of two infrared photons ($^4\text{I}_{15/2} \rightarrow ^4\text{I}_{11/2} \rightarrow ^4\text{F}_{7/2}$) promotes Er^{3+} into $^4\text{F}_{7/2}$ state. Alternatively, in the ETU process a mutual interaction between two Er^{3+} ions previously excited to $^4\text{I}_{11/2}$ leads to de-excitation of one of the ions to the ground state while the other one is promoted to $^4\text{F}_{7/2}$. After the excitation of Er^{3+} into $^4\text{F}_{7/2}$ by either of the mechanisms, non-radiative transition to $^4\text{S}_{3/2}$ ($^4\text{S}_{3/2} + ^2\text{H}_{11/2}$) and the emission occurs.

The mechanism of the red anti-Stokes band often involves non-radiative transition $^4\text{S}_{3/2} \rightarrow ^4\text{F}_{9/2}$. However, taking into account the phonon energy of $\beta\text{-PbF}_2$ crystal, which is estimated as 250 cm^{-1} ,^[10] 10–11 phonons are required to $^4\text{S}_{3/2} \rightarrow ^4\text{F}_{9/2}$ transition. The number of the phonons is too high for this transition to be efficient^[22] and it is unlikely to play a major role in the population of $^4\text{F}_{9/2}$. In our case, the population of the red emitting level probably involves several consecutive cross-relaxation (CR) processes.

The efficacy of the up-conversion and CR is related to the decrease in the distance between the Er^{3+} ions compared to the initial glass, and, correspondingly, to an increase in the ion–ion interaction. Thus it is shown that Er^{3+} ions effectively intercalate into fluoride crystallites with partial crystallization of glass.

4. Conclusions

Eu- and Er-doped glass-ceramics with a cubic crystalline phase were obtained in lead–barium fluoroborate systems. The GC material was transparent in visible and near IR regions. Calculation of the lattice parameters of the crystallites and analysis of the photoluminescence spectra (including the anti-Stokes for Er^{3+}), showed that RE have been efficiently intercalate into cubic fluoride crystallites.

Acknowledgements

This research was financially supported by the Ministry of Education and Science of the Russian Federation by within the framework of basic component of the State Assignment 17.1.18.0026.01 (10.4702.2017/BC).

Conflict of Interest

The authors declare no conflict of interest.

Keywords

barium fluoride, erbium, europium, fluoroborate glass, lead fluoride, luminescence, solid solutions

Received: June 30, 2017

Revised: October 27, 2017

Published online:

- [1] L. C. Courrol, L. R. P. Kassab, V. D. D. Cacho, S. H. Tatum, N. U. Wetter, *J. Luminesc.* **2003**, 102–103, 101.
- [2] W. A. Pisarski, L. Grobelny, J. Pisarska, R. Lisiecki, G. Dominiak-Dzik, W. Ryba-Romanowski, *Laser Phys.* **2010**, 20, 649.
- [3] D. R. Rao, G. S. Baskaran, R. V. Kumar, N. Veeraiyah, *J. Non-Cryst. Sol.* **2013**, 378, 265.
- [4] O. B. Petrova, A. V. Popov, V. E. Shukshin, Y. K. Voron'ko, *J. Opt. Tech.* **2011**, 78, 30.
- [5] K. Biswas, A. D. Sontakke, R. Sen, K. Annapurna, *J. Fluoresc.* **2012**, 22, 745.
- [6] O. B. Petrova, T. S. Sevostjanova, M. O. Anurova, A. V. Khomyakov, *Opt. Spectr.* **2016**, 120, 260.
- [7] J. Weber, *Optical Properties of Ions in Crystals* (Eds: H. M. Crosswhite, H. W. Moose), Interscience, New York **1967**, 467 p.
- [8] V. A. Aseev, E. V. Kolobkova, Ya. A. Nekrasova, N. V. Nikonorov, A. S. Rokhrmin, *Mater. Phys. Mechanics* **2013**, 17, 135.
- [9] B. Szpikowska-Sroka, N. Pawlik, L. Zur, R. Czoik, T. Goryczka, W. A. Pisarski, *Mater. Chem. Phys.* **2016**, 174, 138.
- [10] F. Zeng, G. Ren, X. Qiu, Q. Yang, J. Chen, *J. Non-Cryst. Solids* **2008**, 354, 3428.
- [11] D. N. Karimov, N. I. Sorokin, S. P. Chernov, B. P. Sobolev, *Crystallogr. Rep.* **2014**, 59, 928.
- [12] Y. S. Kuz'minov, *Lithium Niobate Crystals*. Cambridge Int Science Publishing, Cambridge **1999**, 140 p.
- [13] P. P. Fedorov, A. A. Luginina, A. I. Popov, *J. Fluorine Chem.* **2015**, 172, 22.
- [14] B. I. Galagan, I. N. Glushchenko, B. I. Denker, Yu. L. Kalachev, V. A. Mikhailov, S. E. Sverchkov, *Glass Phys. Chem.* **2011**, 37, 258.
- [15] A. A. Kipriyanov, N. G. Karpukhina, *Glass Phys. Chem.* **2006**, 32, 1.
- [16] B. Hatta, M. Tomozawa, *J. Non-Cryst. Solids* **2008**, 354, 3184.
- [17] I. I. Buchinskaya, P. P. Fedorov, *Rus. Chem. Rev.* **2004**, 73, 371.
- [18] M. J. Weber, *Optical Properties of Ions in Crystals*. (Eds: H. M. Crosswhite, H. W. Moose), Interscience, New York **1967**, 467 p.
- [19] A. F. Kirby, F. S. Richardson, *J. Phys. Chem.* **1983**, 87, 2544.
- [20] T. S. Sevostjanova, E. V. Zhukova, O. B. Petrova, A. V. Khomyakov. *Uspehi v himii i himicheskoy tehnologii*, XXIX (3), 64 (2015) (in Russian).
- [21] A. Sarakovskis, G. Kriek. *J. Europ. Ceram. Soc.* **2015**, 35, 3665.
- [22] A. Shalav, B. S. Richards, M. A. Gree, *Sol. Energy Mater. Sol. Cells* **2007**, 91, 829.